Exacta
ISSN: 1678-5428
exacta@uninove.br
Universidade Nove de Julho
Brasil

Chaves, Carlos Alberto; Alves Correa, Valesca; Rui Camargo, José; Nicolini do Patrocinio Nunes, Luiz Eduardo; Queiróz Lamas, Wendell de
Turbulent mixed flow applying CFD in electronic cooling
Exacta, vol. 9, núm. 2, 2011, pp. 261-266
Universidade Nove de Julho
São Paulo, Brasil

Available in: http://www.redalyc.org/articulo.oa?id=81021138011

How to cite
Complete issue
More information about this article
Journal's homepage in redalyc.org

Scientific Information System
Network of Scientific Journals from Latin America, the Caribbean, Spain and Portugal
Non-profit academic project, developed under the open access initiative

DOI: 10.5585/Exacta.v9i2.2743

Turbulent mixed flow applying CFD in electronic cooling

Fluxo turbulento misto aplicando CFD em refrigeração de eletrônicos

Carlos Alberto Chaves
Professor Assistente Doutor do Departamento de Engenharia Mecânica.
Universidade de Taubaté – UNITAU.
Taubaté, SP [Brasil]
chaves@unitau.br

Valesca Alves Correa
Professor Assistente Doutor do Departamento de Engenharia Mecânica.
Universidade de Taubaté – UNITAU.
Taubaté, SP [Brasil]
valesca@unitau.br

José Rui Camargo
Professor Assistente Doutor do Departamento de Engenharia Mecânica.
Universidade de Taubaté – UNITAU.
Taubaté, SP [Brasil]
rui@unitau.br

Luiz Eduardo Nicolini do Patrocinio Nunes
Professor Assistente Doutor do Departamento de Engenharia Mecânica.
Universidade de Taubaté – UNITAU.
Taubaté, SP [Brasil]
luiz@unitau.br

Wendell de Queiróz Lamas
Bolsista CNPq de Pós-doutorado – Grupo de Otimização de Sistemas Energéticos – Departamento de Energia.
Universidade Estadual Paulista – UNESP.
Guaratinguetá, SP [Brasil]
wendell@feg.unesp.br

Abstract

The commercial application CFX® v. 10.0 was used to assess the thermal parameters of electronic devices in which several speed values were explored in a model with a turbulent mixed forced cooling flow. The finite-volume method was used to solve the problem equations throughout the physical domain with the standard k-ϵ turbulence model. It was observed that the maximum temperature is not affected by influence of heat flux in the laminar and turbulent fluxes until heat flux equal 1,000 and maximum dimensionless temperature increase abruptly with heat flux to laminar and turbulent flows for injection dimensionless velocity equal 1, 2, 4, 6, 8, and 10. The results obtained allowed identifying the highest temperature when the system is submitted to combine forced and free convection, making possible to apply control actions, avoiding thermal damages to the devices that work with this cooling process.

Key words: CFD. Electronic devices cooling. Mixed turbulent flow. Numerical analyses.

Resumo

O aplicativo comercial CFX® v. 10.0 foi utilizado para analisar os parâmetros térmicos em equipamentos eletrônicos em que diversos valores de velocidade foram explorados em um modelo com um fluxo de resfriamento turbulento misto forçado. O método de volumes finitos foi utilizado para resolver as equações do problema em todo o domínio físico com o modelo de turbulência k-padrão ϵ. Foi observado que a temperatura máxima não é afetada pela influência do fluxo de calor em fluxos laminar e turbulento até que o fluxo de calor seja igual a 1.000 e a temperatura adimensional máxima aumente abruptamente com o fluxo de calor para as vazões laminar e turbulenta para injeção da velocidade adimensional igual a 1, 2, 4, 6, 8 e 10. Os resultados obtidos permitem identificar a maior temperatura quando o sistema é submetido para combinar convecção livre e forçada, tornando possível aplicar ações de controle, evitando danos térmicos aos dispositivos que trabalham nesse processo de resfriamento.

Palavras-chave: Análise numérica. CFD. Fluxo turbulento misto. Resfriamento de equipamentos eletrônicos.

1 Introduction

The heat transfer in enclosures has been studied for several engineering applications. Results have been presented in research surveys such as in Bruchberg et al. (1976), Kakaç et al. (1987), and it has become a main topic in convective heat transfer textbooks (BEJAN, 1984). Usually the enclosures are closed and natural convection is the single heat transfer mechanism. However, there are several applications in passive solar heating, energy conservation in building and cooling of electronic equipment, in which open cavities are applied (PENOT, 1982; HESS; HENZE, 1984; CHAN; TIEN, 1985). Ramesh and Merzkirch (2001) present a study of steady, combined laminar natural convection and surface radiation from side-vented open cavities with top opening; Gunes and Liakopoulos (2003) study present a spectral element method: the three-dimensional free convection in a vertical channel with spatially periodic, flush-mounted heat sources; Cheng and Lin (2005) present an optimization method of thermoelectric coolers using genetic algorithms and Vasiliev (2006) presents a short review on the micro and miniature heat pipes used as electronic component coolers. Devices applied for the cooling of electronic equipments are frequently based on forced convection (SPARROW et al., 1985). Altemani and Chaves (1988) present a numerical study of heat transfer inside a semi porous two-dimensional rectangular open cavity for both local and average Nusselt numbers at the heated wall and for the isotherms and streamlines of the fluid flowing inside the open cavity. Bessaih and Kadja (2000) described a numerical simulation of conjugate, turbulent natural convection air cooling of three heated components mounted on a vertical channel and showed the study of reduced temperatures. Silva et al. (2007) presented a work about a numerical analysis of the heat transfer inside a semi porous two-dimensional rectangular open cavity, where forced and natural convection were considered.

This paper presents a continued work (SILVA et al., 2007) where about a turbulent numerical analysis of the heat transfer inside a semi porous three-dimensional rectangular open cavity. This is made by two vertical parallel plates opened at the top and closed at the bottom by a uniform heat flow, as indicated in Figure 1. One of the vertical plates is porous and there is a normal forced fluid flow passing through. The opposite vertical plate supplies the same uniform heat flow to the cavity. In addition to the forced convection, the analysis considered the influence of natural convection effects. The maximum temperatures were obtained for the uniformly heated plate and to the bottom for the parameters like injection velocity and heat flow.

This study can be applied in many industrial applications such as solar heating, energy conservation in buildings, refrigeration of electronic equipment and other systems in which heat transfer occurs by forced convection. So, for cooling purposes, the results obtained allowed identifying the highest temperature when the system is submitted to combined forced and free convection, making possible to apply control actions, avoiding thermal damages to the devices that work with this cooling process.

1.1 Analysis

The conservation equations of mass, momentum and energy, as well as their boundary conditions, will be expressed for the system indicated in Figure 1. One of the vertical plates is porous and there is a normal forced fluid flowing through it. The opposite vertical plate supplies the same uniform heat flow to the cavity: a uniform tempera-

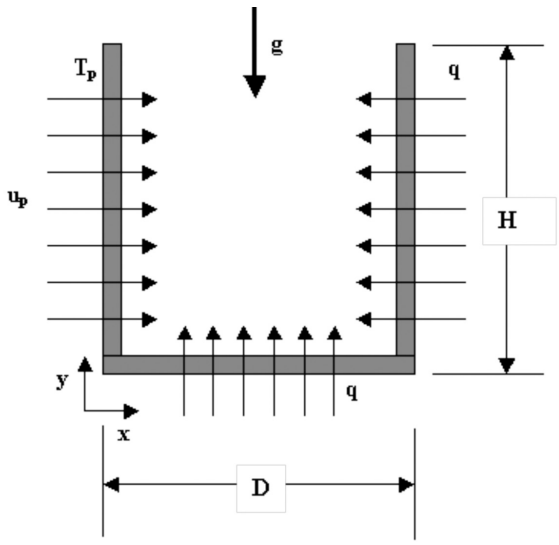

Figure 1: Coordinate system and thermal boundary conditions of the open cavity

ture at the porous wall and a specified heat flow at the heat vertical wall an in the bottom.

For an incompressible fluid, with constant thermo-physical properties, except for variation of density with temperature in the buoyancy force term (i.e. the Boussinesq approach is valid), the governing equations for turbulent flow can be written in non-dimensional form as bellow.

In order to obtain the conservation equations in dimensionless form, the following variables were defined, where the components of the velocity are *U*, *V*, and *W*:

$$X = \frac{x}{D}; \quad Y = \frac{y}{D} \tag{1a}$$

$$U = u \cdot \frac{D}{\nu}; \quad V = v \cdot \frac{D}{\nu} \tag{1b}$$

$$P = \frac{p^*}{\left(\frac{\rho \cdot \nu^2}{H^2}\right)}; \quad \theta = \frac{T - T_p}{\left(\frac{q \cdot D}{k}\right)} \tag{1c}$$

Continuity equation

$$\frac{\partial U}{\partial X} + \frac{\partial V}{\partial Y} = 0 \tag{2}$$

Momentum equation in X direction

$$\frac{\partial (UU)}{\partial X} + \frac{\partial (VU)}{\partial Y} = -\frac{\partial P}{\partial X} + Pr\left\{\frac{\partial}{\partial X}\left[(\nu^* + \nu_y^*)\frac{\partial U}{\partial X}\right] + \frac{\partial}{\partial Y}\left[(\nu^* + \nu_t^*)\frac{\partial U}{\partial Y}\right]\right\} \tag{3}$$

Momentum equation in Y direction

$$\frac{\partial (UV)}{\partial X} + \frac{\partial (VV)}{\partial Y} = -\frac{\partial P}{\partial Y} + Pr\left\{\frac{\partial}{\partial X}\left[(\nu^* + \nu_y^*)\frac{\partial V}{\partial X}\right] + \frac{\partial}{\partial Y}\left[(\nu^* + \nu_t^*)\frac{\partial V}{\partial Y}\right]\right\} + Ra \cdot Pr \cdot \theta \tag{4}$$

Energy equation

$$\frac{\partial (U\theta)}{\partial X} + \frac{\partial (V\theta)}{\partial Y} = \left\{\frac{\partial}{\partial X}\left[(k^* + \alpha_y^*)\frac{\partial \theta}{\partial X}\right] + \frac{\partial}{\partial Y}\left[(k^* + \alpha_t^*)\frac{\partial \theta}{\partial Y}\right]\right\} + S \tag{5}$$

Turbulent kinetic energy equation

$$\frac{\partial (UK)}{\partial X} + \frac{\partial (VK)}{\partial Y} = Pr \cdot \left\{\frac{\partial}{\partial X}\left[\left(\nu^* + \frac{\nu_t^*}{\sigma_k}\right)\frac{\partial K}{\partial X}\right] + \frac{\partial}{\partial Y}\left[\left(\nu^* + \frac{\nu_t^*}{\sigma_k}\right)\frac{\partial K}{\partial Y}\right]\right\} + Pr \cdot \nu_t^*\left[\left(\frac{\partial U}{\partial Y} + \frac{\partial V}{\partial X}\right)^2 + 2 \cdot \left(\frac{\partial U}{\partial X}\right)^2 + 2 \cdot \left(\frac{\partial V}{\partial Y}\right)^2\right] - \varepsilon - Ra\frac{Pr^2}{Pr_t}\nu_t^*\frac{\partial \theta}{\partial Y} \tag{6}$$

Rate of turbulent kinetic energy dissipation equation

$$\frac{\partial (U\varepsilon)}{\partial X} + \frac{\partial (V\varepsilon)}{\partial Y} = Pr \cdot \left\{\frac{\partial}{\partial X}\left[\left(\nu^* + \frac{\nu_t^*}{\sigma_\varepsilon}\right)\frac{\partial \varepsilon}{\partial X}\right] + \frac{\partial}{\partial Y}\left[\left(\nu^* + \frac{\nu_t^*}{\sigma_\varepsilon}\right)\frac{\partial \varepsilon}{\partial Y}\right]\right\} + C1 \cdot Pr \cdot \nu_t^* \cdot \frac{\varepsilon}{K} \cdot \left[\left(\frac{\partial U}{\partial Y} + \frac{\partial V}{\partial X}\right)^2 + 2 \cdot \left(\frac{\partial U}{\partial X}\right)^2 + 2 \cdot \left(\frac{\partial V}{\partial Y}\right)^2\right] - C2 \cdot \frac{\varepsilon^2}{K} - Ce \cdot Ra \cdot \frac{Pr^2}{Pr_t}\nu_t^*\frac{\varepsilon}{K}\frac{\partial \theta}{\partial Y} \tag{7}$$

In Equations (2) to (9), T_p indicates the temperature of the fluid inlet at the porous wall and the scales used for the non-dimensioning of length, time, velocity, pressure, temperature, kinetic energy and dissipation are: D, D^2/α, α/D, $\rho(\alpha/D)^2$, QD^2/k_s, $(\alpha/D)^2$, α^3/D^4, respectively. *Ra* and *Pr* are the Rayleigh and Prandtl numbers, defined respectively as:

$$Ra = \frac{g\beta\left[qD^2 / k_s\right]}{\alpha\nu} \tag{8}$$

$$Pr = \frac{\nu}{\alpha} \tag{9}$$

where q is the heat density, k_S the thermal conductivity of heated components, g the magnitude of gravitational acceleration, β the thermal expansion coefficient of the fluid, ρ its density, ν the kinematics viscosity and α the thermal diffusivity. The non-dimensional viscosity ν^* is ν/ν_{air} and is equal to 1 in the fluid region and ∞ within the solid regions corresponding to components. The non-dimensional turbulent eddy viscosity ν^*_t is $(C_\mu/Pr)\ K^2/\epsilon$ in the fluid domain and zero within the solid regions. The non-dimensional thermal conductivity is $k^*=k/k_{air}$, the non-dimensional turbulent thermal diffusivity α^*_t is $(Pr/Pr_t)\ \nu^*_t$.

The constants of the standard k–ϵ model are those given by Jones and Launder (1981) and are: $C1$=1.44; $C2$=1.92; C_μ=0.09; σ_ε=1.00; σ_k=1.30; and Pr_t=1.00. The constant C_e in the buoyant term of the dissipation equation was chosen as 0.70.

At the three solid boundaries of the open cavity, the velocity components are null, except the velocity of injection of the fluid (Up) at the porous wall. The thermal boundary conditions comprise a uniform (reference) temperature at the porous wall and a specified heat flow at the heated vertical wall and in the bottom. Expressed in dimensionless terms, the boundary conditions become:

$$X=0; U_p = u_p \frac{D}{\nu} = Re_p; V=0, \theta = 0 \tag{10a}$$

$$X=1;\ U=0;\ V=0,\ \frac{\partial\theta}{\partial X}=1 \tag{10b}$$

$$Y=0;\ U=0;\ V=0,\ \frac{\partial\theta}{\partial Y}=1 \tag{10c}$$

where Rep is the porous wall Reynolds number.

The equations of the turbulent kinetic energy and its dissipation, Equations (6) and (7), were solved only in the fluid region. The turbulent kinetic energy is set to zero at solid walls, and its normal gradients are prescribed as zero at the other boundaries. The equation of dissipation is not solved at nodes that are adjacent to the wall.

2 Material and methods

The methodology consists in solving the physical problem using the finite volume CFD code CFX® v. 10.0 from Ansys to discretize the three-dimensional partial differential equations of the mathematical model (PATANKAR, 1980). Scalar quantities (P, θ, k and ϵ) are stored in the centre of these volumes, whereas the components of the velocity (U, V, and W) are stored on the faces. Power law profiles are used for the dependent variables to ensure realistic results.

Convergence of the numerical solution at consecutive time steps was reached when the mass, momentum and energy residuals were chosen after performing grid independence tests for a mesh with 12,062 nodes and 63,984 tetrahedral elements. It is considered a goal error equal to 10^{-3} for mass flow, velocity, turbulence and turbulent dissipation energy in CFX® v. 10.0.

For the simulation of cooling process it was used an electronic cooling with dimensions listed in Table 1.

Table 1: Values used to computational simulation

Propriety	Value
Width	0,1 [m]
Height	0,1 [m]
Depth	1 [m]
Air inlet temperature	25 [°C]
Atmospheric pressure	101,32 kPa

3 Results and discussion

Figure 2 express the results of maximum temperature inside cavity in function of injection dimensionless velocity Up and heat flow parameters in the surface to laminar and turbulent flows. The effect of heat flow in the behavior of maximum dimensionless temperature is shown on Figure 2 for injection velocity Up equal 1, 2, 4, 6, 8 and 10. It is evident that the maximum dimensionless temperature is affected by heat flow by influence of forced convection to laminar and turbulent flows. Until heat flow equal 1,000 the maximum dimensionless temperature is not affected by heat flow by influence of forced convection to laminar and turbulent flows. After 1,000 the maximum dimensionless temperature is affected by influence of heat flow for injection dimensionless velocity Up equal 1, 2, 4, 6, 8 and 10. After heat flow equal 1,000, the maximum dimensionless temperature increases abruptly with heat flow to laminar and turbulent flows for injection dimensionless velocity Up equal 1, 2, 4, 6, 8, and 10.

4 Conclusion

The mathematical model development was applied with techniques of computational fluid dynamic (CFD) and a cooling process with specified dimensions and defined geometry. The simulations of this process were performed with the commercial software CFX® v. 10.0 to evaluate the maximum dimensionless temperature in relation to the air flow through an electronic device inside the cavity of laminar and turbulent fluxes. It was observed the maximum dimensionless temperature was not affected by influence of heat flow in the laminar and turbulent fluxes until heat flow equal 1,000. It was also observed that maximum dimensionless temperature increase abruptly with heat flow of laminar and turbulent flows for injection velocity Up equal 1, 2, 4, 6, 8, and 10. Considering the range for injection velocity Up, it can be seen that the influence of heat flow is stronger than forced convection after heat flow equal 1,000. So, for cooling purposes, the results obtained allowed identifying the highest temperature when the system is submitted to combine forced and free convection, making possible to apply control actions, avoiding thermal damages to the devices that work with this cooling process.

References

ALTEMANI, C. A. C.; CHAVES, C. A. Convective cooling of a semiporous open cavity. In: XXVI NATIONAL HEAT TRANSFER CONFERENCE, HEAT TRANSFER IN ELECTRONICS – HTD. 1988. *Proceedings*... Philadelphia: ASME, v. 111, 1988. p. 149-154.

BEJAN, A. *Convection heat transfer*. New York, NY: Wiley Interscience, 1994.

BESSAIH, R.; KADJA, M. Turbulent natural convection cooling of electronic components mounted on a vertical channel. *Applied Thermal Engineering*, v. 20, p. 141-154, 2000.

BRUCHBERG, H. et al. Natural convection in enclosed spaces: a review of applications to solar energy collection. *ASME Journal of Heat Transfer*, v. 98, p. 182-188, 1976.

CHAN, Y. L.; TIEN, C. L. A numerical study of two-dimensional laminar natural convection in shallow open cavities. *International Journal of Heat Mass Transfer*, v. 28, p. 603-612, 1985.

CHENG, Y.; LIN, W. Geometric optimization of thermoelectric coolers in a confined volume using genetic algorithms. *Applied Thermal Engineering*, v. 25, p. 2983-2997, 2005.

GUNE, H.; LIAKOPOULOS, A. Three-dimensional convective cooling in a vertical channel with flush-mounted heat sources. *International Journal of Heat and Mass Transfer*, v. 46, p. 791-808, 2003.

HESS, C. F.; HENZE, R. H. Experimental investigation of natural convection losses from open cavities. *ASME Journal of Heat Transfer*, v. 106, p. 33-338, 1984.

JONES, W. P.; LAUNDER, B. E. The calculation of low-reynolds number phenomena with a two-equation model of turbulence. *International Journal of Heat Mass Transfer*, v. 16, p. 1119-1130, 1981.

KAKAÇ, S. et al. *Handbook of single phase convective heat transfer*. New York: J. Wiley, 1987.

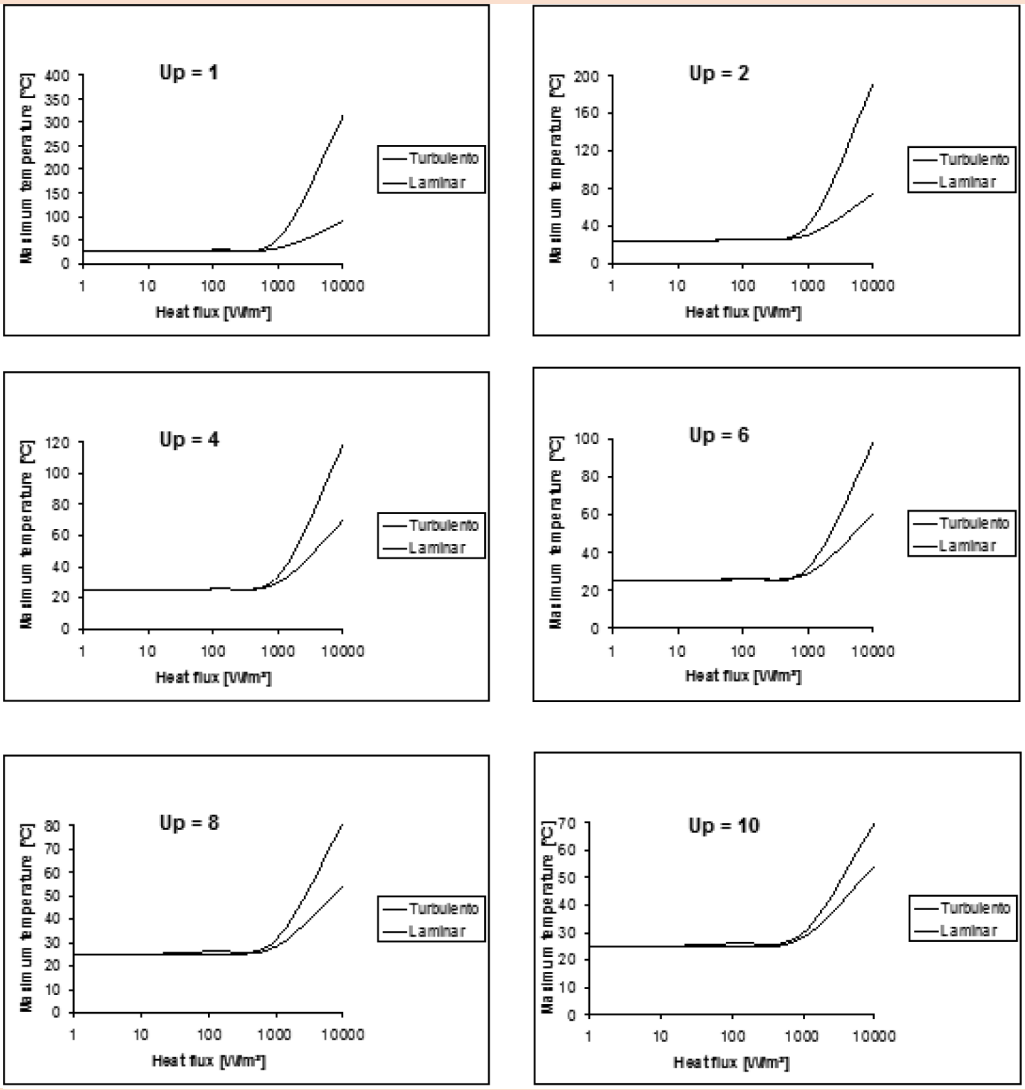

Figure 2: Laminar and turbulent representation to heat flow and maximum temperature to velocity Up to 1, 2, 4, 6, 8, and 10

PATANKAR, S. V. *Numerical heat transfer and fluid flow*. Hemisphere: McGraw-Hill, 1980.

PENOT, F. Numerical calculation of two-dimensional natural convection in isothermal open cavities. *Numerical Heat Transfer*, v. 5, p. 421-437, 1982.

RAMESH, N.; MERZKIRCH, W. Combined convective and radiative heat transfer in side-vented open cavities. *International Journal of Heat and Fluid Flow*, v. 22, p. 180-187, 2001.

SPARROW, E. M. et al. Heat transfer and pressure drop in flow passages that open along their lateral edges. *International Journal of Heat Mass Transfer*, v. 28, n. 4, p. 731-740, 1985.

SILVA, M. N. et al. Convective cooling of electronic equipment. In: XIX International Congress of Mechanical Engineering – COBEM, 2007, Brasília. *Proceedings*... Brasília, DF: ABCM, 2007.

VASILIEV, L. L. Micro and miniature heat-pipes: electronic component coolers. *Applied Thermal Engineering*, article in press, 2006.

Recebido em 29 abr. 2011 / aprovado em 29 jun. 2011

Para referenciar este texto
CHAVES, C. A. et al. Turbulent mixed flow applying CFD in electronic cooling. *Exacta*, São Paulo, v. 9, n. 2, p. 261-266, 2011.